

Anomalous diffraction profiles of alkali-halide-alkali-cyanide mixed crystals

K. Knorr, Alois Loidl

Angaben zur Veröffentlichung / Publication details:

Knorr, K., and Alois Loidl. 1986. "Anomalous diffraction profiles of alkali-halide-alkali-cyanide mixed crystals." *Physical Review Letters* 57 (4): 460–62.
<https://doi.org/10.1103/physrevlett.57.460>.

Nutzungsbedingungen / Terms of use:

licgercopyright

Dieses Dokument wird unter folgenden Bedingungen zur Verfügung gestellt: / This document is made available under these conditions:

Deutsches Urheberrecht

Weitere Informationen finden Sie unter: / For more information see:

<https://www.uni-augsburg.de/de/organisation/bibliothek/publizieren-zitieren-archivieren/publiz/>



Anomalous Diffraction Profiles of Alkali-Halide-Alkali-Cyanide Mixed Crystals

K. Knorr and A. Loidl

Institut für Physik, Universität Mainz, Mainz, Federal Republic of Germany

(Received 6 March 1986)

The x-ray diffraction profiles of four mixed alkali halides-alkali cyanides have been studied. At the threshold concentration where the systems change over from ferroelastic ordering to the glass state, the profiles are highly unusual. The diffracted intensity of transverse scans along the cubic axes follows $I \sim \exp(-\alpha|\xi|)$, where ξ is the reduced wave vector, measured from the line center.

PACS numbers: 64.70.Kb, 61.10.-i, 64.70.Pf

The mixed alkali halides-alkali cyanides like $(\text{KBr})_{1-x}(\text{KCN})_x$ show a strong decrease of the elastic shear constant with decreasing temperature.^{1,2} Above a threshold concentration x_c this softening leads to ferroelastic transitions into noncubic crystalline phases³; for concentrations below x_c the resulting low-temperature state is characterized by inhomogeneous strain fields and static random CN orientations.^{1,4} This so-called glass state is an object of high current interest as it evolves continuously out of a crystalline (cubic) phase and combines properties of the spin-glasses and of the conventional glasses. There is no doubt that the softening of the lattice is due to a linear coupling between the CN orientations and the phonons. For concentrated systems ($x=1$) in the cubic phase a detailed theory has been developed.⁵ The understanding of the mixed crystals is still insufficient because the concept of a "virtual crystal" is—quite obviously—not applicable for intermediate concentrations. Other concepts like "frustration" or "random fields" seem adequate but are not yet cast into a quantitative form.

In this situation we recently directed attention to a more general, dimensional aspect²: The mixed cyanides with concentrations $x \geq x_c$ seem to be—experimental evidence was given for $(\text{KBr})_{0.27}(\text{KCN})_{0.73}$ —the first examples of the $m=2$ universality class for ferroelastic transitions.^{6,7} For such systems the softening of the shear modes at the critical temperature is predicted to go hand in hand with a divergence of the mean square displacement,⁷ which means that the crystalline order is destroyed. There are two ways in which the system can cope with this disordered state. It can conserve it and form a glass down to lowest temperature, or it can pass into the ferroelastic low-temperature phase by recrystallization. Obviously the cyanides choose either way depending on whether x is smaller or larger than x_c . This view puts the cyanides in the more general frame of crystallization versus glass formation.

In the present article x-ray diffraction data are reported for a cyanide mixed crystal which is exactly at x_c , namely $(\text{KCl})_{0.2}(\text{KCN})_{0.8}$. This statement stems

from the following experimental observation: Powdered samples and small single crystals have been taken from the same part of a larger crystal. The powders showed a coexistence of orthorhombic diffraction lines with broadened, glasslike cubic lines below 100 K,⁸ whereas in the small single crystals the ferroelastic ordering was completely suppressed. Complementary data on $(\text{KBr})_{1-x}(\text{KCN})_x$, $x=0.40, 0.53, 0.73$, will be mentioned as examples for systems which are somewhat away from x_c (for the bromides x_c is about 0.62).

So far neutron diffraction patterns of the glass state of the bromides with $x=0.50$ and 0.53 have been studied by Rowe *et al.* and by Loidl *et al.*,⁴ respectively. The pioneering work of Rowe *et al.* documents the appearance of anisotropic disorder scattering, the central peak of the inelastic-neutron-scattering profiles, which is strongest in the T_{2g} scattering geometry. The results have been interpreted in terms of a crystalline model.⁵ Loidl *et al.* observed that the widths of the Bragg reflections increase with $|\mathbf{Q}|^3$, where \mathbf{Q} is the scattering vector, and claimed that this dependence is incompatible with a crystalline lattice.

The single crystals have been grown by S. Haussühl, Universität zu Köln, with the exception of the $x=0.40$ bromide, which was purchased from the Crystal Growth Laboratory of the University of Utah. It was specified to be $x=0.50$. The concentrations given here are derived from the macroscopic density. The room-temperature fcc lattice parameters are 6.473 ± 0.004 Å for the chloride, and 6.546, 6.560, and 6.570 Å for the bromides with $x=0.73, 0.53$, and 0.40, respectively. The x-ray experiments have been performed on a conventional two-circle diffractometer, with use of Cu $K\alpha$ radiation reflected from a (002) graphite monochromator. The samples have been cleaved from large crystals. Samples with obvious misoriented grains have been rejected. It turned out that the requirement of clean cubic room-temperature lines of high intensity and hence a high dynamic reserve could be met only for the ($h00$) reflections of relatively large crystals (3–5 mm³). Here the radiation is reflected from the cleavage faces in a specular way.

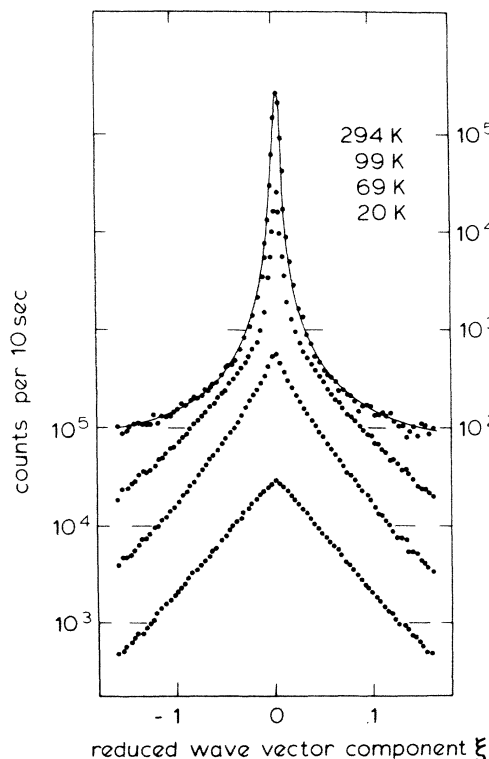


FIG. 1. The $(2\xi 0)$ profiles of $(\text{KCl})_{0.2}(\text{KCN})_{0.8}$ shown on a logarithmic intensity scale. The left scale refers to the 20-K data, and the right one to the 294-K data. The profiles are shifted by one order of magnitude with respect to each other. The ticks mark the 10^3 level for each run. The solid line of the high-temperature profile results from the superposition of a δ -like Bragg spike and diffuse intensity $I \sim \xi^{-2}$, folded with the experimental resolution and fitted to the data. The linewidth at 294 K is 0.0057 in ξ or 0.17° in the rocking angle (FWHM).

In addition it is only in this series that three nodes ($h=2, 4, 6$) could be reached. The $(h00)$ lines have been studied down to the lowest temperatures by performing, in particular, transverse scans along $[010]$. For these reflections the experimental resolution is defined by the size of the reflecting facet (typically $1.5 \times 1.5 \text{ mm}^2$) and by the entrance and exit slit with a horizontal width of 0.2 mm and a vertical width of 2 mm, at a distance of 250 mm from the sample.

Figure 1 shows the $(2\xi 0)$ profile of the chloride at several temperatures. A more detailed T dependence of the diffracted intensity at two special Q values is presented in Fig. 2. The low-temperature profiles of all three $(h00)$ nodes are shown in Fig. 3. The profiles down to about 150 K are well described by a δ -like Bragg spike plus a diffuse intensity I originating from the long-wavelength acoustic phonons, folded with the three-dimensional resolution ellipsoid (Fig. 1, solid line); at sufficiently large ξ values I is proportional to ξ^{-2} . As T decreases further the Bragg component

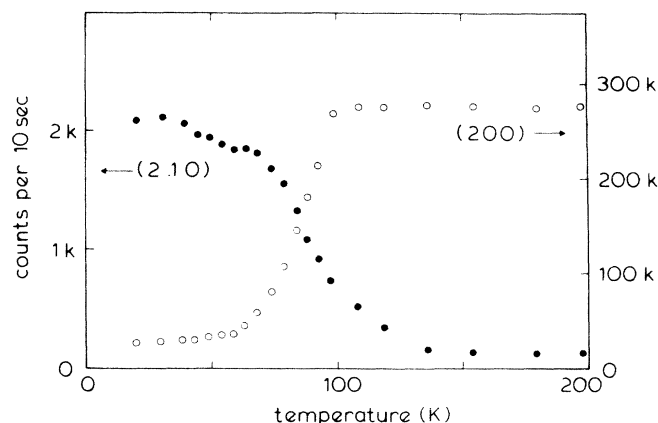


FIG. 2. The temperature dependence of the diffracted intensity at (200) and (2.10) of $(\text{KCl})_{0.2}(\text{KCN})_{0.8}$.

decreases and the diffuse component increases, finally yielding a profile of the form $I \sim \exp(-\alpha|\xi|)$, where the decay parameter depends on the order of the node: $\alpha = 26.7 \pm 0.2$ for $h=2$, 9.2 ± 0.2 for $h=4$, and 4.9 ± 0.3 for $h=6$. The residual rounding at $\xi=0$ is due to resolution effects. For the (200) low-temperature profile the exponential decay could be traced over two and a half orders of magnitude until the intensity settles at the background counting rate. This unusual line shape does not seem to be a special feature of the chloride, since trends towards this type of profile have been observed in the bromides, too. Figure 4 shows the low-temperature diffraction patterns of the glass state of the $x=0.53$ bromide. The data on the bromide with $x=0.73$ just above the ferroelastic ordering temperature look very similar. It is only for the lower concentration, $x=0.40$, that none of the nodes shows the exponential-decay-type profile.

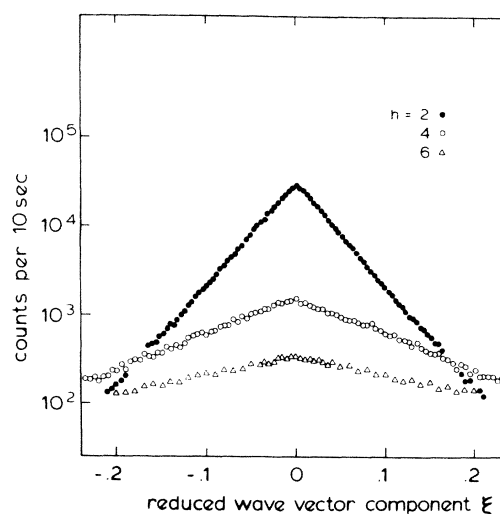


FIG. 3. The $(h\xi 0)$ profiles for $h=2, 4, 6$ of $(\text{KCl})_{0.2}(\text{KCN})_{0.8}$ at 20 K. The actual counting time per step was 10 sec for $h=2, 4$, and 30 sec for $h=6$.

Obviously this shape occurs for concentrations close to x_c only. In all samples the longitudinal scans along $(2 + \xi 00)$ remain sharp.

A structure factor exponentially decaying in reciprocal space is, to our knowledge, novel. It is startling by its general shape and by its nonanalytic behavior at $\xi = 0$. There is a crystalline aspect to it since the cusps at $\xi = 0$ define points in reciprocal space which form a lattice (as far as one can say from the small number of nodes studied), in very much the same way as the Bragg spikes of a crystal do. On the other hand, the patterns have a different shape at different nodes— α depends on h —whereas in a crystal they would be identical in every Brillouin zone apart from a scale factor slowly varying with Q . On the whole, the replacement of the strong δ -like Bragg singularities by weaker cusplike singularities at the nominal reciprocal lattice points is not unexpected in a situation where the mean square displacement is supposed to diverge.

There is no straightforward interpretation of these patterns. Referring to fluctuations in crystals one is used to an Ornstein-Zernike behavior with an exponential decay of the correlation function in real space and a Lorentzian-shaped structure factor in reciprocal space (including the special case of long-wavelength elastic fluctuations where $I \sim \xi^{-2}$). Deviations from this behavior are known to occur in several situations: (i) at critical points where the algebraic part of the spatial correlation function dominates, (ii) in systems at the lower marginal dimension, e.g., in two-dimensional solids where $I \sim \xi^{-2+\eta}$ holds,^{9,10} and (iii) at phase transitions in the presence of random fields, where the structure factor is treated as the sum of a Lorentzian and a squared Lorentzian.¹¹ An attempt was made to fit the structure factors pertinent to these situations to the present data, but none give a good description over an appreciable temperature range, let alone explain the variation of the diffraction pattern with the node index h .

Furthermore, we tried to relate the profiles to models of imperfect lattices, a lattice subject to distributions of strains¹² and a perturbed and a paracrystalline lattice.¹³ The two latter models differ in the point of whether the deviation of a cell from its position in an underlying perfect lattice is bound or cumulative. The diffracted intensity can be written as a series expansion, a Fourier expansion for the strain model and an expansion into Airy-type functions for the two other models. Applied to the present case these series will be long, if not infinite, and the physical significance of the decomposition is by no means obvious. For the strain model, for example, the partial information on the strain distribution which can be derived from three nodes only definitely rules out a Gaussian-shaped distribution, which would have been the most natural first guess.

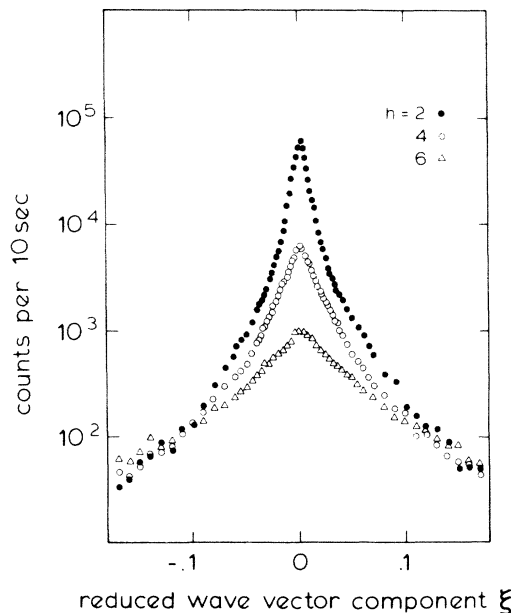


FIG. 4. The $(h\xi 0)$ profiles, $h=2, 4, 6$, of $(\text{KBr})_{0.47}(\text{KCN})_{0.53}$ at 12 K. The actual counting time per step was 5 sec for $h=2$, 10 sec for $h=4$, 30 sec for $h=6$. At 297 K the ξ width of the (200) reflection was 0.0038 (FWHM).

Thus we can only speculate that the present diffraction profiles are due to a yet unknown superposition of strains, those connected with the size and shape and possibly the domain microstructure of the sample and random strains originating from the chemical disorder, both types of strain enhanced by the unusual softness of the elastic shear constant.

We are grateful to Professor S. Haussühl who generously supplied the samples.

¹J. M. Rowe, J. J. Rush, D. G. Hinks, and S. Susman, Phys. Rev. Lett. **43**, 1158 (1979).

²K. Knorr, A. Loidl, and J. K. Kjems, Phys. Rev. Lett. **55**, 2445 (1985).

³K. Knorr and A. Loidl, Phys. Rev. B **31**, 5387 (1985).

⁴A. Loidl, M. Müllner, G. McIntyre, K. Knorr, and H. Jex, Solid State Commun. **54**, 367 (1985).

⁵K. H. Michel and J. M. Rowe, Phys. Rev. B **22**, 1417 (1980).

⁶R. A. Cowley, Phys. Rev. B **13**, 4877 (1976).

⁷R. Folk, H. Iro, and F. Schwabl, Z. Phys. B **25**, 69 (1976), and Phys. Rev. B **20**, 1229 (1979).

⁸E. Civera-Garcia, K. Knorr, A. Loidl, and S. Haussühl, to be published.

⁹B. Jancovici, Phys. Rev. Lett. **19**, 20 (1967).

¹⁰Y. Imry and L. Gunther, Phys. Rev. B **3**, 3939 (1971).

¹¹R. J. Birgeneau, H. Yoshizawa, R. A. Cowley, G. Shirane, and H. Ikeda, Phys. Rev. B **28**, 1438 (1983).

¹²B. E. Warren and B. L. Averbach, J. Appl. Phys. **21**, 595 (1950).

¹³T. R. Welberry, Rep. Prog. Phys. **48**, 1543 (1985).